J. Eng. Technol. Sci., Vol. 53, No. 6, 2021, 210607

Pitting Corrosion in AA7075 Friction Stir Welds on Minor Additions of Silver

Kodamasimham Sri Ram Vikas[1,*], Vuppala Sesha Narasimha Venkata Ramana[2], Koona Bhavani[2], Challa Kishore Reddy[1], & Vadapalli Srinivas[2]

[1]Department of Mechanical Engineering, Prasad V. Potluri Siddhartha Institute of Technology, Vijayawada 520007, Andhra Pradesh, India
[2]Department of Mechanical Engineering, GITAM (Deemed to be University), Visakhapatnam 530045, Andhra Pradesh, India
*E-mail: sriramvikas@gmail.com

Highlights:

- Pitting corrosion resistance increased in AA7075 FS welds by incorporating silver
- Pit density of silver added AA7075 FS welds is lower
- Tool rotation speed influences the grain size and silver dissemination
- Hardness in TMAZ and HAZ decreased due to coarse precipitates

Abstract. AA7075 is extensively used in aerospace, defense, automotive applications because of its high strength to weight ratio. Issues related to fusion welding and corrosion resistance are key problems associated with these alloys. Friction stir welding is an alternative welding technique that overcomes problems associated with fusion welding. In the present investigation, preliminary studies were done on pitting corrosion behavior of AA7075 friction stir welds by adding silver along the weld joint line. Silver paste was applied along the longitudinal direction of AA7075-T6 rolled plates of 6-mm thickness and cured at 130 °C for 30 seconds. Weld joints were prepared at two different tools rotational speeds, i.e., 750 rpm and 1000 rpm, while keeping other parameters fixed. Welded joints were cut as per the required sizes to study the hardness, microstructure, and pitting corrosion resistance in various regions. It was observed that the hardness was not much affected, but pitting corrosion resistance substantially improved by trace addition of silver. In the stir zone and the thermo-mechanically affected zone, onion ring type marks were observed. Grain refinement in the stirred zone (SZ) was higher at 750 rpm compared to 1000 rpm. The increased hardness in the welds was due to grain refinement. All the observed results were correlated with microstructural features as evidenced by optical microscopy.

Keywords: *AA7075; friction stir welding; microstructure; pitting corrosion resistance; silver.*

Received July 20th, 2020, 1st Revision October 22nd, 2020, 2nd Revision February 3rd, 2021, Accepted for publication November 30th, 2021.
 ISSN: 2337-5779, DOI: 10.5614/j.eng.technol.sci.2021.53.6.7

1 Introduction

AA7075 (Al-Zn-Mg-Cu) is exclusively used in aerospace applications due to its high strength to weight ratio and effective response to age-hardening behavior [1]. The key problem associated with this alloy is that fusion welding is not possible – although welding is done – because changes in microstructure in the heat-affected zone (HAZ) and porosity in fusion zone (FZ) lead to a substantial reduction in mechanical properties [2,3]. An alternative joining technique for overcoming problems that are associated with fusion welding (FW) is friction stir welding (FSW), which is a solid-state joining process. Typically, it is an inherent hot working process and the temperature during the welding process never goes beyond $0.8T_m$ [4]. Less residual stresses and distortions are the advantages of FSW as compared with conventional fusion welding techniques [5]. Another major problem associated with fusion welding of AA7075 alloy is its sensitiveness towards corrosion resistance. It has been reported in the early 1960s that exfoliation corrosion is associated with a light gauge plate and is preferential along grain boundaries [1].

In AA7075, intermetallic precipitates cause corrosion [6]. Typically, in these alloys, $MgZn_2$ precipitates are highly anodic and are responsible for corrosion. Another important aspect of the corrosion of these alloys are precipitate free zones (PFZs) [7]. In Al-Zn-Mg alloys, depletion of Zn and Mg at PFZs gives rise to higher electric potential as compared in grains. Moreover, the $MgZn_2$ precipitates possess low potential and due to this difference between $MgZn_2$ precipitates and PFZs preferential dissolution occurs [8]. In order to mitigate the corrosion of AA7075 alloys, several researchers have adopted various techniques like solution treatment [9], aging treatment, retrogression, and re-aging (RRA) [10, 11]. Some researchers have tried to incorporate ceramic and alloy powders such as nano B_4C, TiC, α-β titanium by FSW, and friction stir processing (FSP) techniques to improve corrosion resistance [12-14].

Very few investigators have studied the corrosion behavior of Al-Ag alloys. From the literature, it is evident that the age hardening of Al-Alloy produces silver-rich intermetallic precipitates in the matrix and these precipitate sites favor the generation of oxygen [15]. This results in the formation of Ag_2O and the clusters of oxidized Ag will be deposited on an anodic film without enrichment. Ag^+ ions migrate faster than Al^{3+} ions in Al-Ag alloy [16]. In Al-Ag alloy, Ag_2Al precipitates are formed, called γ phase, which are responsible for a decrease in corrosion resistance of the alloy. These precipitates produce local galvanic cells and prolonged aging leads to more development of these precipitates, which further reduces corrosion resistance [17]. However, the addition of silver in AA7075 can improve corrosion resistance. Silver has a high solubility in aluminum. Minor addition of silver increases the strength as well as stress

corrosion cracking (SCC) resistance in this alloy. It is typically added in the range of 0.1 to 0.6 wt.% [18]. The addition of trace silver enhances the ageing hardening behavior. Welded Al-Zn-Mg alloy also shows improved resistance to SCC. Around grain boundaries, interactions between silver and magnesium atoms and vacant lattice sites lead to promotion of precipitation by modifying the structure and typically $MgZn_2$ (η') precipitates are increased by nucleation [19]. It also restricts the formation of PFZs [20]. It is well known that in these alloys, η' precipitates dissolve preferentially along grain boundaries. Presence of silver resists SCC in Al-Zn-Mg-Cu and Al-Zn-Mg alloys by coexisting with $MgZn_2$ (η') precipitates and it also decreases the potential that is associated with PFZs and subdues the anodic dissolution of η' precipitates. The presence of high potential Ag in the grains leads to less potential difference. This suppresses the leaching grain boundaries. To understand this phenomenon, a more detailed investigation is needed [21]. In Al-Zn-Mg alloy, the addition of silver causes pronounced curtailment or else total elimination of PFZs around grain boundaries and defects that are responsible for SCC. This effect is more pronounced when the alloy is rapidly quenched. Even keeping the alloy at higher aging temperatures and using prolonged aging times also reduces the susceptibility towards SCC [22]. The addition of Ag beyond 0.6 wt.% causes more sensitivity towards quenching, which reduces the strength. Addition of 0.2 wt.% Ag is a candidate that does not compromise strength [23]. In the present work, a novel technique was applied for incorporating silver into AA7075 welds. The scope of this work was to study the effect of silver on the corrosion resistance of AA7075 friction stir (FS) welds.

2 Experimental Details

AA7075-T6 rolled plates of size (300 × 150mm) and thickness 6 mm were cut into the required size (150 × 150 mm) using a hydraulic power hacksaw machine. The chemical composition and mechanical properties of the base alloy are presented in Tables 1 and 2 respectively. These plates were cleaned using acetone, followed by drying. Along the edge of the longitudinal direction, commercial silver paste (supplied by M/S Technistro, Nagpur) of 200 nm particle size, was applied and these plates were kept in an electric oven at 130 °C for 30 seconds for curing of the paste. A BISS-ITW 3-axis friction stir welding machine was used for joining these plates. A schematic of the process of FSW is shown in Figure 1. A H13 heat-treated tool with hardness 60 HRC was used; the tool dimensions are shown in Figure 2. The joints were made using two different tool rotational speeds viz. 750 rpm and 1000 rpm, while keeping the other parameters constant. Detailed process parameters are presented in Table 3 and Figure 3 shows the FS welded AA7075-T6 plates. After completion of welding, the welded plates were cut using a wire cut electric discharge machine (WEDM) into required dimensions for microstructure analysis, and microhardness and pitting corrosion tests.

Table 1 Chemical composition of base metal AA7075-T6 in wt.%.

Element	Si	Fe	Cu	Mn	Mg	Cr	Zn	Ti	Al
Actual value	0.04	0.22	1.66	0.02	2.58	0.21	5.75	0.03	Balance

Table 2 Mechanical properties of base metal AA7075-T6.

Material	Tensile Strength (MPa)	Yield Strength (MPa)	Elongation (%)	Vickers Hardness (VHN)
Base material (AA7075-T6)	579	512	12	175

Table 3 FSW parameters used in the fabrication of AA7075-T6 joints.

Process parameters	Setup 1	Setup 2
Tool rotational speed (rpm)	750	1000
Welding speed (mm/min)	40	40
Plunging force (kN)	10	10
Initial heating time (sec)	3	3
Tool depth (mm)	5.5	5.5
Tilt angle	2°	2°

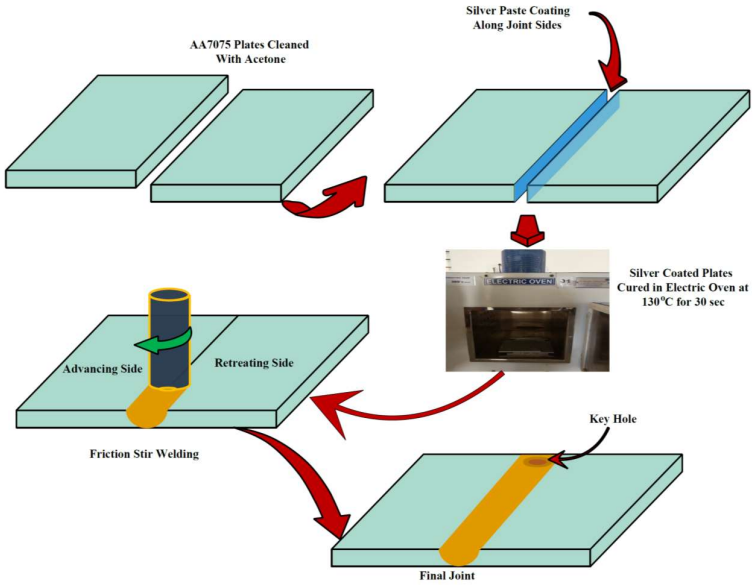

Figure 1 Schematic of friction stir welding process of silver-coated AA7075-T6 plates.

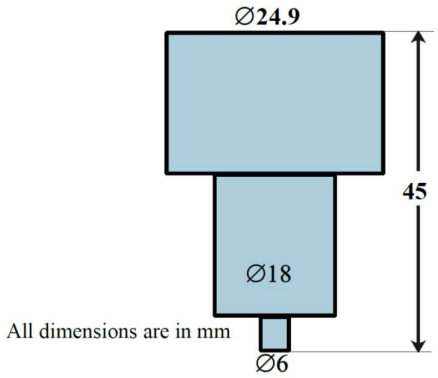

Figure 2 Friction stir welding tool dimensions.

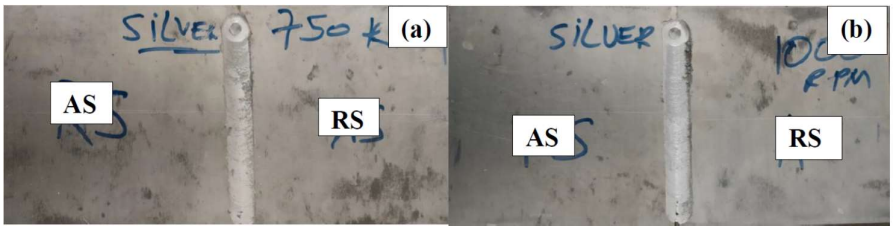

Figure 3 AA7075-T6 plates friction stir welded at different spindle speeds: (a) 750 rpm, (b) 1000 rpm. AS refers to advanced side and RS refers to retreat side.

For metallographic examination, the specimens were cleaned using a wire brush, followed by acetone cleaning. Later, the specimens were polished by using SiC emery papers ranging from 240 to 1000 grit, followed by disc polishing using alumina powder. Keller's etchant of composition (distilled water190 ml, nitric acid 5 ml, hydrochloric acid 3 ml, hydrofluoric acid 2 ml) was applied for 10 seconds and dried. Optical microstructures at different regions of the weld were observed by using Leica CTR 6000 optical microscope.

2.1 Mechanical Properties Evaluation

Vickers microhardness test (ASTM E 384) was carried out on base metal (BM), stir zone (SZ), and thermo-mechanically affected zone (TMAZ)/HAZ of the weld specimen with 300 gf load, and 15 seconds dwelling time. 5 readings were taken; the average hardness values are reported in Section 3 (Results and Discussion).

2.2 Electrochemical Corrosion Tests

Electrochemical corrosion tests evaluate the pitting corrosion resistance of aluminum alloys and their welds. This is done in terms of electrochemical corrosion potential (ECP) measured during a potentiodynamic polarization test and was conducted here as per the ASTM G 69 standard. The ECP of a material is estimated by exposing the selected surface of the material to an aqueous solution of 3.5% sodium chloride (NaCl) mixed with H_2O_2. This solution acts as a cathodic reactant; its pH is adjusted to 10 throughout the experiment. Saturated calomel electrode (SCE) is used as a reference electrode and a carbon electrode is used as an auxiliary electrode.

A potential scan was carried at a rate of 0.166 mV/sec until pitting started at an initial potential of -0.25 V (OC) SCE, which is called the final potential. Calculation of critical pitting potential (E_{pit}) is done when the current increases at a particular potential. When a test specimen exhibits comparatively more positive potential (or less negative potential) its pitting corrosion resistance is considered to be improved. In order to study the pitting corrosion behavior of BM, SZ and TMAZ/HAZ zones of the welds, the Gill AC basic electrochemical system software was used. As the TMAZ/HAZ is very small in size, it is difficult to test the TMAZ and HAZ exclusively; hence, the TMAZ with HAZ was exposed to the electrolyte as a combined zone during the corrosion test.

3 Results and Discussion

3.1 Microstructure Studies

Energy dispersive X-ray spectroscopy (EDS) confirmed the elements in AA7075 and silver coated AA7075 to be Mg, Zn, Cu, Ag (Figure 4). The optical microstructure (OM) of the AA7075 is shown in Figure 5. Grain boundary precipitate eutectics of $MgZn_2$ (dark spots) were observed in and around grain boundaries. These are called M phase [24-26]. Typically, the microstructure also reveals some intermetallics in grains. These intermetallics have been previously studied and identified as Al_7Cu_2Fe, $(Al, Cu)_6(Fe, Cu)$, [11].

The OMs of the various zones in the FS welds joined at a spindle speed of 750 rpm and 1000 rpm with and without the addition of silver are presented in Figures 6 to 9. From these micrographs the various zones present in the FS welds are clearly evident. In SZ, fine and equiaxed recrystallized grains were observed, which are due to tool stirring action and temperature (Figures 7(b) and 9(b)). Grains in other regions were not finer in size as compared with SZ. In the as-received base material, grain sizes of 50 to 60 μm were observed and in SZ the

grain size ranged from 6 to 14 µm. In the TMAZ region, the grain sizes were in the range of 20 to 30 µm.

The grain size was not much affected in the HAZ; it was 50 µm, which is close to BM. Onion ring type marks were observed in the SZ as well as in the TMAZ. Tool rotational speed affects the microstructure. A high rotational speed leads to an increase in the temperature gradient, which widens the HAZ and also causes grain coarsening, dissolution, and accumulation of hardening precipitates near grain boundaries [27].

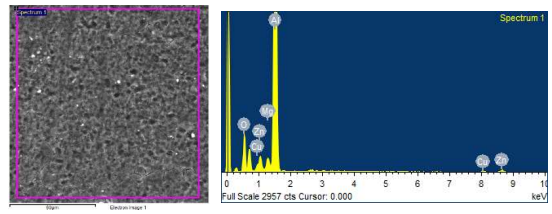

Element	Weight%	Atomic%
O K	27.64	40.12
Mg K	1.71	1.63
Al K	65.58	56.44
Cu K	1.55	0.57
Zn K	3.52	1.25
Totals	100.00	

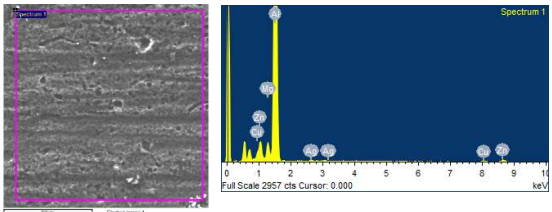

Element	Weight%	Atomic%
Mg K	2.41	2.78
Al K	90.58	94.24
Cu K	1.51	0.67
Zn K	5.23	2.25
Ag L	0.28	0.07
Totals	100.00	

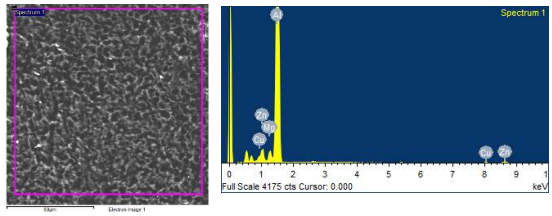

Element	Weight%	Atomic%
Mg K	2.32	2.68
Al K	90.91	94.40
Cu K	1.81	0.80
Zn K	4.96	2.12
Totals	100.00	

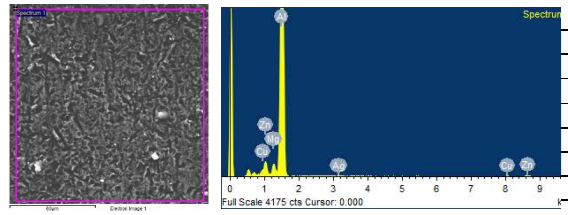

Element	Weight%	Atomic%
Mg K	2.27	2.63
Al K	90.55	94.34
Cu K	1.68	0.74
Zn K	5.03	2.16
Ag L	0.47	0.12
Totals	100.00	

Figure 4 EDS of friction stir welded AA7075 stir zone: (a) 750 rpm, (b) silver coated 750 rpm, (c) 1000 rpm, (d) silver coated1000 rpm.

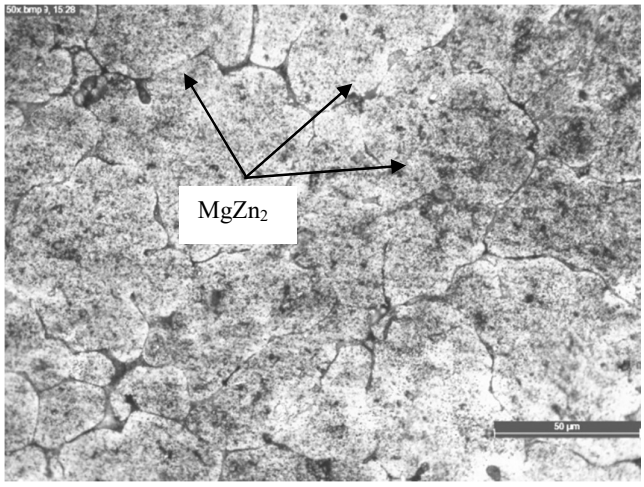

Figure 5 Optical microstructure of AA7075.

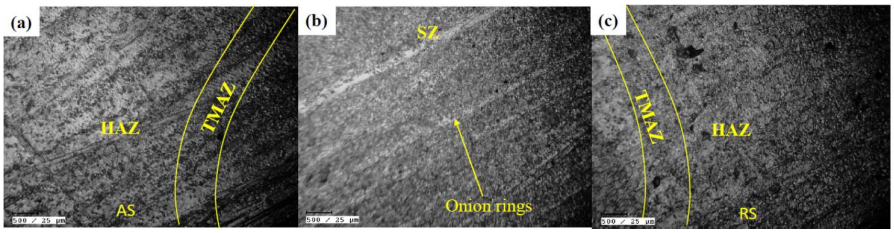

Figure 6 Optical micrographs of AA7075-T6 plates friction stir welded at 750 rpm: (a) advancing side, (b) stir zone, (c) retreating side. Magnification 500×.

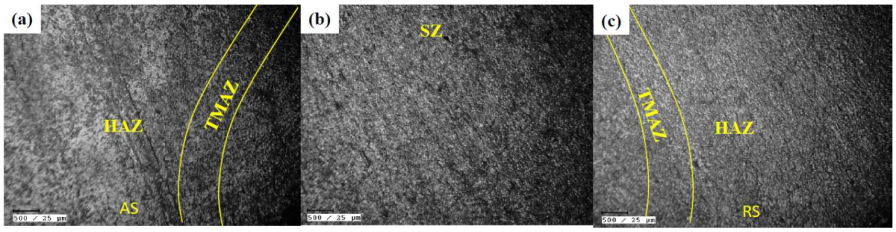

Figure 7 Optical micrographs of AA7075-T6 friction stir welded silver-coated at 750 rpm (a) Advancing side (b) stir zone (c) Retreating side. Magnification 500×.

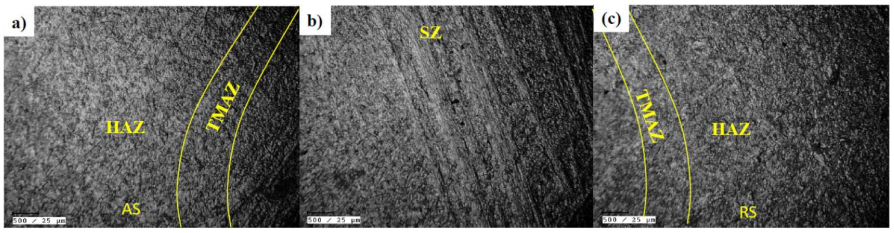

Figure 8 Optical micrographs of AA7075-T6 friction stir welded at 1000 rpm: (a) advancing side, (b) stir zone, (c) retreating side. Magnification 500×.

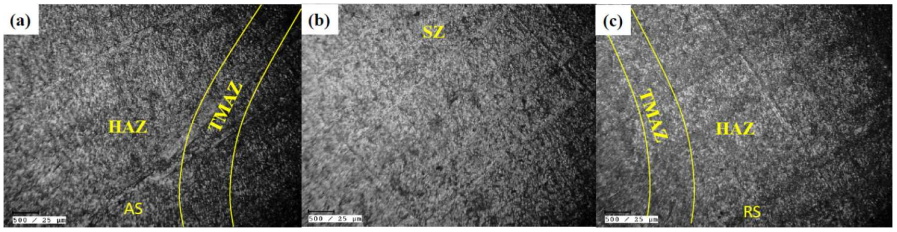

Figure 9 Optical micrographs of friction stir welded silver-coated AA7075-T6 at 1000 rpm: (a) advancing side, (b) stir zone, (c) retreating side. Magnification 500×.

3.2 Microhardness Studies

The microhardness values were measured at various points, starting from the weld center and towards the TMAZ, the HAZ and the base metal on both the advancing and retreating sides of the welded joint. The hardness profile of the welded joints at different rotational speeds and in various zones are presented in Figure 10. The hardness measurements were taken on top of the weld surface. From Figure 10 it is observed that when the plates were FS welded at 750 rpm spindle speed, the hardness values were higher when compared to the values for a spindle speed of 1000 rpm. This is attributed to the ultrafine grain structure obtained in the welds when spindle speed is 750 rpm (Figure 7(b)). Golezani, *et al.* [28] has reported similar observations, where grain size depends on rotational speed and high rotational speeds lead to high heat input developing, resulting in a coarse grain structure, which subsequently affects the hardness. As we know from the Hall-Petch equation, grain size influences the hardness of a material; it decreases with increasing grain size. From Figure 10 it can clearly be seen that in various zones the hardness decreased subsequently from the SZ to the HAZ because of an increase in grain size. In TMAZ hardness was lower because this zone contains partially recrystallized grains, which are larger than SZ and smaller than HAZ.

This decrease in hardness widened to the transition regions of the TMAZ and the HAZ. Hardness reduction was observed in the HAZ, which is due to the coarsening of precipitates. In the HAZ, reduction in hardness was observed because of the dissolution of strengthening precipitates ($MgZn_2$) and similar observations have been reported by Linton & Ripley [29]. The presence of η′ precipitates in the BM region increased the hardness [30-31]. In the silver-coated FS welded plates, the hardness slightly improved at 750 rpm because silver promotes nucleation of $MgZn_2$ precipitates [19] and due to the presence of an ultra-fine grain structure in SZ and also smaller grain sizes in other regions as compared with SZ and other regions of silver-coated FS welded with a spindle speed of 1000 rpm (Figure 9).

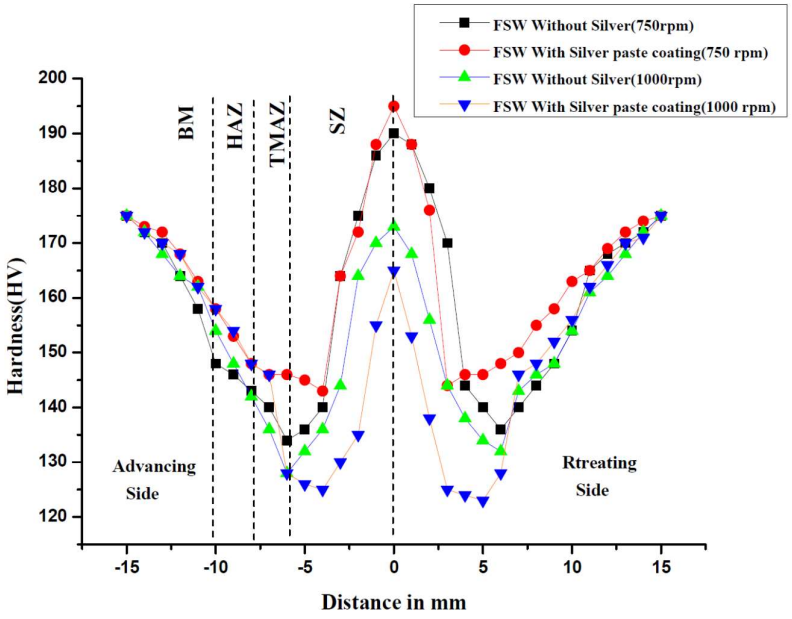

Figure 10 Comparison of the hardness of AA7075-T6 friction stir welded at 1000 rpm and 750 rpm spindle speeds with and without the addition of a silver coating.

3.3 Pitting Corrosion Studies

Pitting corrosion is attributed to the difference in potential between the matrix and grain boundary precipitates and can be determined by microstructural changes, precipitates, PFZs and solute concertation gradients. In AA7075, corrosion occurs due to the presence of $MgZn_2$ precipitates, which are anodic. These precipitates promote the susceptibility towards pitting corrosion [32]. The pitting corrosion potential values of various zones in the FS welds for 750 rpm

and 1000 rpm spindle speeds and with and without the addition of silver are presented in Table 4. The pitting potential (E_{pit}) (mV) values in different regions clearly show a significant increase in corrosion resistance at the stir zone of the FS welds with the addition of silver at both spindle speeds (Table 4).

The addition of a silver coating helped in the proper dissemination of silver particles in the SZ of the welds, which in turn protects the matrix grains from corrosion. It is clearly understood from previous studies that silver promotes $MgZn_2$ precipitates and also envelops these precipitates. This decreases the potential and lowers the anodic dissolution of these η′ precipitates [21]. Base metal susceptibility towards pitting corrosion is high because it is very well known that η′ precipitates are more concentrated in T6 condition [33]. In the 750 rpm FS welded plates, corrosion resistance at the SZ was low as compared with the SZ in the 1000 rpm FS welded plate. This is because higher spindle speeds lead to coarser grains [34]. Moreover, it is well known that coarser grains have less galvanic coupling [35]. Even in the TMAZ/HAZ curves of the FS welded plates the same was observed (Figures 11 and 12). Meanwhile, in the silver-coated plates welded at 750 rpm, the SZ showed improved pitting corrosion resistance as compared with 1000 rpm because at low speeds silver is likely to be reminded in the stir zone.

It is also evident from previous studies that lower speeds result in a more narrow distribution of particles [36-37]. It is interesting to note that pitting corrosion resistance in the TMAZ/HAZ at 750 rpm was lower than in the TMAZ/HAZ at 1000 rpm. This can be ascribed to the heat input and broader dissemination of particles, as it is known that at high speeds there will be a high heat input, which results in grain coarsening[35]. Furthermore, at high speeds particle dissemination is fast [37],which is why even though grain size was larger in the SZ, corrosion resistance was lower in the FS welded plate at 1000 rpm. Another reason for the lower corrosion resistance in the SZ of the silver-coated plate FS welded at 1000 rpm is that at high heat input the precipitates get coarser, which are anodic in nature [33], and also the presence of silver is less likely, as it is known that particles disseminate at a faster rate at high speeds. These are the reasons for the better corrosion resistance of the SZ (36 mV) with 750 rpm spindle speed welds compared to 1000 rpm spindle speed welds (-55 mV), while better corrosion resistance was observed in the TMAZ/HAZ (-205mV) with 1000 rpm spindle speed welds compared with 750 rpm spindle speed welds (-222 mV).

The potentiodynamic polarization curves shown in Figure 10 and 11 also show the same tendency. The friction stir welds with silver addition show better corrosion resistance than the welds without silver addition. Optical micrographs of weld surfaces after the corrosion test are shown in Figures 13 to 16. In these optical micrographs the pit density in various zones for various conditions of the

welds is clearly visible. As the pitting corrosion was better in the FS welds made at a rotational speed of 750 rpm with the addition silver compared to other conditions and zones, the pit density was also much lower in this zone.

Table 4 Pitting potential (Epit) (mV) values of base metal AA7075-T6 and its friction stir welds in various zones at various spindle speeds.

Base metal/weld	Condition	E_{pit} (mV)	
Base metal	T6	-710	
Friction stir welds at spindle rotational speed (rpm)		SZ	TMAZ/HAZ
750	Friction stir welds without silver paste	- 141	-389
	FS welds with silver paste	36	-222
1000	Friction stir welds without silver paste	- 134	-293
	FS welds with silver paste	-55	-205

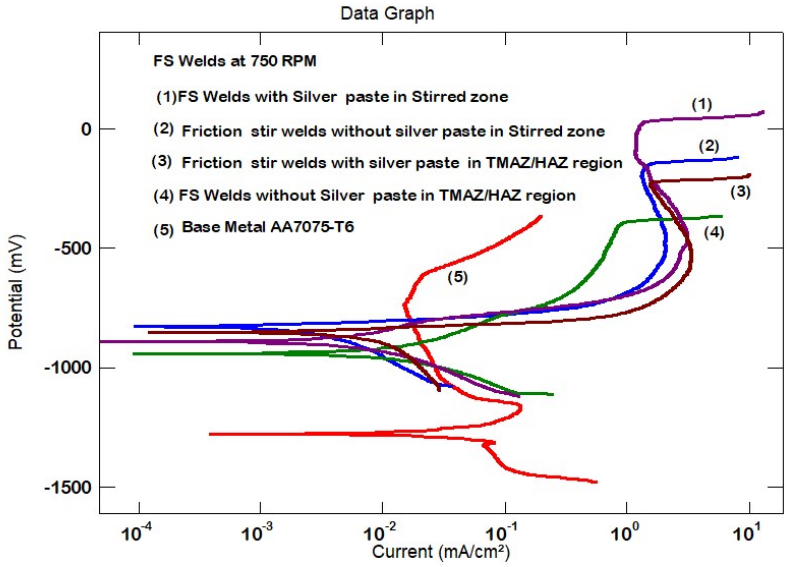

Figure 11 Potentiodynamic polarization curves of AA7075-T6 friction stir welds with and without the addition of silver in the SZ and TMAZ/HAZ at spindle speed 750 rpm.

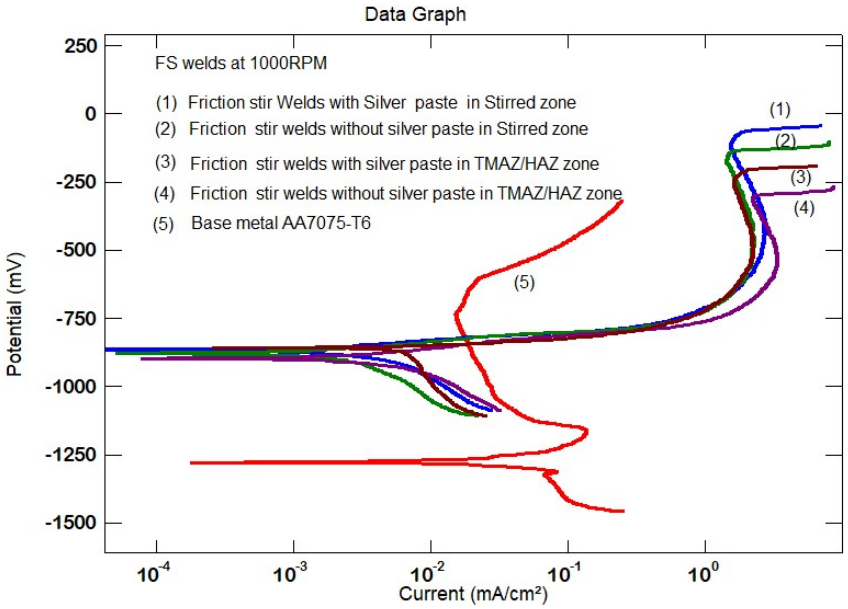

Figure 12 Potentiodynamic polarization curves of AA7075-T6 friction stir welded with and without the addition of silver in the SZ and TMAZ/HAZ at spindle speed 1000 rpm.

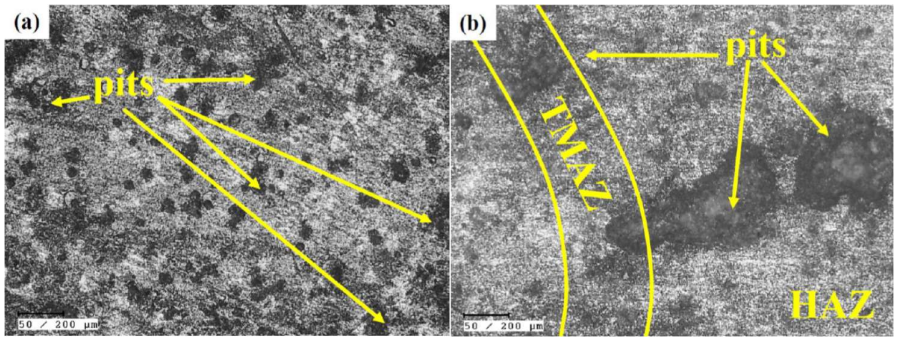

Figure 13 Optical micrographs of AA7075-T6 dynamic polarized friction stir welded at 750 rpm: (a) stir zone, (b) TMAZ/HAZ.

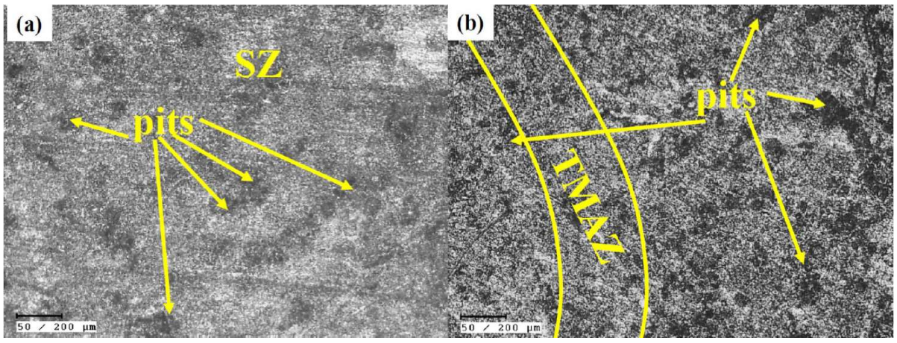

Figure 14 Optical micrographs of AA7075-T6 dynamic polarized friction stir welded silver-coated at 750 rpm (a) Stir zone (b) TMAZ/HAZ.

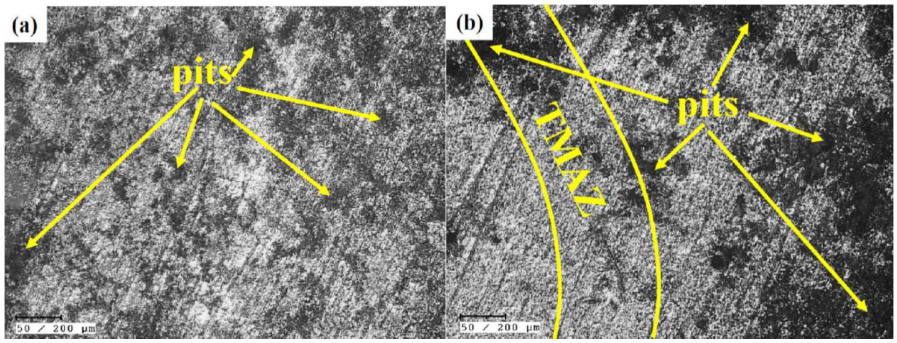

Figure 15 Optical micrographs of AA7075-T6 dynamic polarized friction stir welded at 1000 rpm: (a) stir zone, b) TMAZ/HAZ.

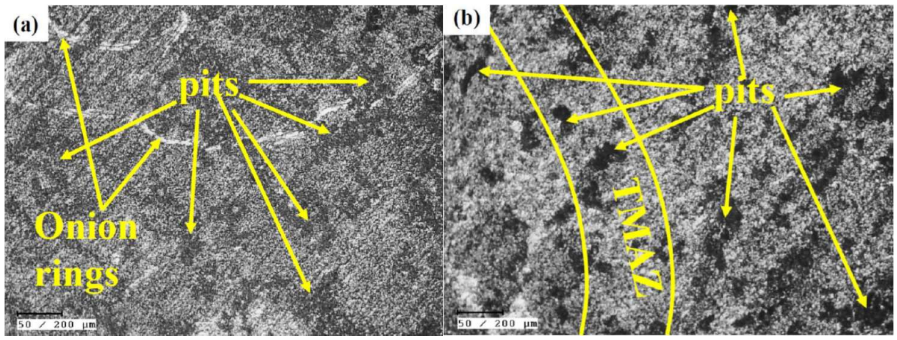

Figure 16 Optical micrographs of AA7075-T6 dynamic polarized friction stir welded silver-coated at 1000 rpm: (a) stir zone, (b) TMAZ/HAZ.

4 Surface Roughness

The surface of the welds after the corrosion test were examined for pit density using a Mitutoyo Surf Test SJ-210 portable surface roughness tester with a sampling cutoff length 0.08 mm. The surface roughness was measured 5 times in each region and the average was taken. Figure 17 shows the surface roughness values of pits in different regions. From these mean roughness depth (RZ) values it is also clear that the addition of silver improved the surface finish, i.e. the corrosion resistance in the welds compared to without the addition of silver.

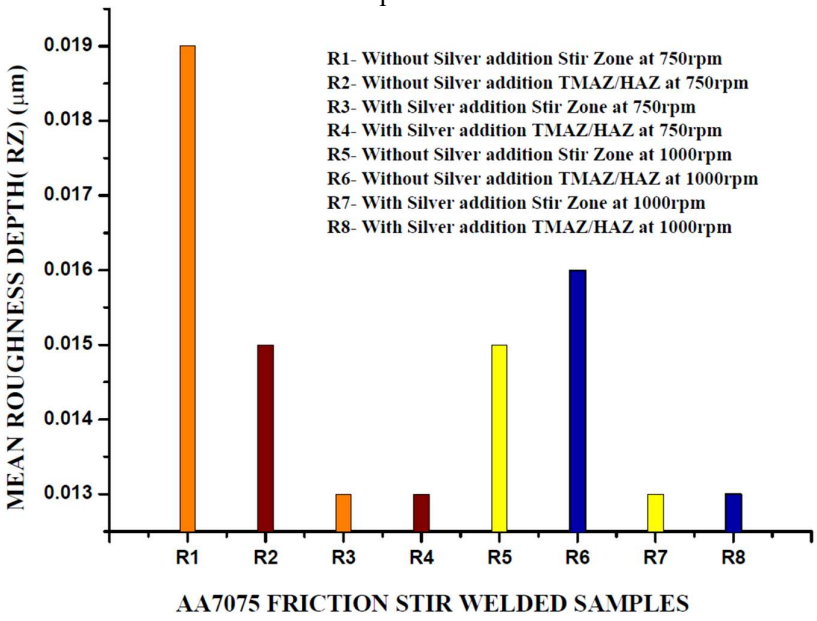

Figure 17 Surface roughness values of dynamic polarized AA7075-T6 friction stir welds with and without silver coating in different zones at different spindle speeds.

5 Conclusions

AA7075 plates were welded with and without the addition of a silver coating at the welded portion using friction stir welding. An onion ring type morphology was observed in the SZ as well as in the TMAZ of the welds. The grains were highly refined when welded at a spindle speed of 750 rpm compared to 1000 rpm. It was found that an increase in the tool rotational speed affected the microstructure, especially widening the HAZ. When the plates were friction stir welded at 750 rpm, the hardness values were higher when compared to 1000 rpm. This is contributed to the ultrafine grain structure obtained in the welds when the

spindle speed was 750 rpm. Overall corrosion resistance was improved in the FS welds with addition of silver both at spindle speed 750 rpm and 1000 rpm. The addition of a silver coating helped in the proper dissemination of silver particles in the SZ of the welds, which in turn protects the matrix grains from corrosion. In the surface roughness tests it was observed that the surface roughness (RZ) of the pit densities of silver added FS welds was lower as compared with the FS welds without silver addition in different regions.

Acknowledgments

The authors gratefully acknowledge the Dr. Sastry S. Indrakanti Group, Department of Metallurgical and Materials Engineering, Rajiv Gandhi University of Knowledge Technologies, Basar, Telangana, India, for granting permission to perform friction stir welding.

References

[1] Staley, J.T., *History of Wrought-Aluminum-Alloy Development*, Aluminum Alloys-Contemporary Research and Applications, **31**, Elsevier, pp. 3-31, 1989.

[2] Nicolas, M. & Deschamps, A., *Characterisation and Modelling of Precipitate Evolution in an Al–Zn–Mg Alloy During Non-Isothermal Heat Treatments*, Acta Mater., **51**(20), pp. 6077-6094, Dec. 2003.

[3] Alatorre, N., Ambriz, R.R., Noureddine, B., Amrouche, A., Talha, A. & Jaramillo, D., *Tensile Properties and Fusion Zone Hardening for GMAW and MIEA Welds of a 7075-T651 Aluminum Alloy*, Acta Metall. Sin. English Lett., **27**(4), pp. 694-704, Jul. 2014.

[4] Venugopal, T, Roa. K.S. & Roa, K.P., *Studies on Friction Stir Welded AA 7075 Aluminium Alloy*, Trans. Indian Inst. Met., **57**(6), pp. 559-663, 2004.

[5] John, R., Jata, K.V. & Sadananda, K., *Residual Stress Effects on Near-threshold Fatigue Crack Growth in Friction Stir Welds in Aerospace Alloys*, in International Journal of Fatigue, 2003, **25**(9-11), pp. 939-948, 2003

[6] Sameljuk, A., Neikov, O., Krajnikov, A., Milman, Y. & Thompson, G., *Corrosion Behaviour of Powder Metallurgical and Cast Al–Zn–Mg Base Alloys*, Corros. Sci., **46**(1), pp. 147-158, Jan. 2004.

[7] Doig, P. & Edington, J.W., *Influence of Precipitate Free Zones on the Stress Corrosion Susceptibility of a Ternary Al-5.9 Wt% Zn-3.2 Wt% Mg Alloy*, Corrosion, **31**(10), pp. 347-352, Oct. 1975.

[8] Shikama, T. & Yoshihara, S., *Highly SCC Resistant 7000-series Aluminum Alloy Extrusion*, Kobelco Technol. Rev., **35**, pp. 65-68, 2017.

[9] Shastry, C.R., Levy, M. & Joshi, A., *The Effect of Solution Treatment Temperature on Stress Corrosion Susceptibility of 7075 Aluminium Alloy*, Corros. Sci., **21**(9-10), pp. 673-688, Jan. 1981.

[10] Yang, W., Ji, S., Zhang, Q. & Wang, M., *Investigation of Mechanical and Corrosion Properties of an Al-Zn-Mg-Cu Alloy under Various Ageing Conditions and Interface Analysis of H' Precipitate*, Mater. Des., **85**, pp. 752-761, Nov. 2015.

[11] Kumar, P.V., Reddy, G.M. & Rao, K.S., *Microstructure, Mechanical and Corrosion Behavior of High Strength AA7075 Aluminium Alloy Friction Stir Welds – Effect of Post Weld Heat Treatment*, Def. Technol., **11**(4), pp. 362-369, Dec. 2015.

[12] Vijaya Kumar, P., Madhusudhan Reddy, G. & Srinivasa Rao, K., *Microstructure and Pitting Corrosion of Armor Grade AA7075 Aluminum Alloy Friction Stir Weld Nugget Zone -Effect of Post Weld Heat Treatment and Addition of Boron Carbide*, Def. Technol., **11**(2), pp. 166-173, Jun. 2015.

[13] Kumar, S., Kumar, A. & Vanitha, C., *Corrosion Behaviour of Al 7075 /Tic Composites Processed Through Friction Stir Processing*, Mater. Today Proc., **15**, pp. 21-29, 2019.

[14] Ikumapayi, O.M. & Akinlabi, E.T., *Efficacy of A-B Grade Titanium Alloy Powder (Ti–6Al–2Sn–2Zr–2Mo–2Cr–0.25Si) in Surface Modification and Corrosion Mitigation in 3.5% Nacl on Friction Stir Processed Armour Grade 7075-T651 Aluminum Alloys - Insight in Defence Applications*, Mater. Res. Express, **6**(7), 076546, Apr. 2019.

[15] Riveros, V., *Influence of Surface Treatments in the Initial Stages of Anodizing Al–Ag Alloys in Neutral Electrolytes*, J. Solid State Electrochem., **10**(2), pp. 83-90, Feb. 2006.

[16] Paez, M.A., *Anodic Oxidation of Al-Ag Alloys*, Corros. Sci., **44**(12), pp. 2857-2863, Dec. 2002.

[17] Afzali, P., Yousefpour, M. & Borhani, E*., Evaluation of the Effect of Ageing Heat Treatment on Corrosion Resistance of Al-Ag Alloy Using Electrochemical Methods*, J. Mater. Res., **31**(16), pp. 2457-2464, Aug. 2016.

[18] Hatch, J.E., *Aluminum: Properties and Physical Metallurgy*, American Society for Metals, 1984.

[19] Polmear, I.J., *The Influence of Small Additions of Silver on the Structure and Properties of Aged Aluminum Alloys*, JOM, **20**(6), pp. 44-51, Jun. 1968.

[20] Ogura, T., Hirosawa, S., Hirose, A. & Sato, T., *Effects of Microalloying Tin and Combined Addition of Silver and Tin on the Formation of Precipitate Free Zones and Mechanical Properties in Al-Zn-Mg Alloys*, Mater. Trans., **52**(5), pp. 900-905, May 2011.

[21] Hirano, M., Kobayasi, K. & Tonda, H., *Effect of the Chemical Composition on the Mechanical Properties and Stress Corrosion Cracking Sensitivities of High-Strength Al-Zn-Mg Alloy*, J. Soc. Mater. Sci. Japan, **49**(1), pp. 86-91, 2000.

[22] Mondolfo, L.F., *Aluminum Alloys: Structure and Properties*, London: Butterworths, 1976.

[23] Hirano, M., Kobayasi, K. & Tonda, H., *Effect of the Additional Element on the Weldability of High-Strength Al-Zn-Mg Alloy*, J. Soc. Mater. Sci. Japan, **49**(1), pp. 92-97, 2000.

[24] Isadare, A.D., *Effect of Heat Treatment on Some Mechanical Properties of 7075 Aluminium Alloy*, Materials Research, **16**(1), pp. 190-194, 2013.

[25] Lotfi, Amir, H. & Nourouzi, S., *Effect of Welding Parameters on Microstructure, Thermal, And Mechanical Properties of Friction-Stir Welded Joints of AA7075-T6 Aluminum Alloy*, Metallurgical and Materials Transactions A, **45**(6), pp. 2792-2807, 2014.

[26] Sudhakar, I., *Enhancement of Wear and Ballistic Resistance of Armour Grade AA7075 Aluminium Alloy Using Friction Stir Processing*, Defence Technology, **11**(1), pp. 10-17, 2015.

[27] Rezaei, H., Mirbeik, M.H. & Bisadi, H., *Effect of Rotational Speeds on Microstructure and Mechanical Properties of Friction Stir-Welded 7075-T6 Aluminium Alloy*, Proc. Inst. Mech. Eng. Part C J. Mech. Eng. Sci., **225**(8), pp. 1761-1773, 2011.

[28] Golezani, A.S., Barenji, R.V., Heidarzadeh, A. & Pouraliakbar, H., *Elucidating of Tool Rotational Speed in Friction Stir Welding of 7020-T6 Aluminum Alloy*, Int. J. Adv. Manuf. Technol., **81**(5-8), pp. 1155-1164, Nov. 2015.

[29] Linton, V.M. & Ripley, M.I., *Influence of Time on Residual Stresses in Friction Stir Welds in Agehardenable 7xxx Aluminium Alloys*, Acta Mater., **56**(16), pp. 4319-4327, Sep. 2008.

[30] Rajakumar, S., Muralidharan, C. & Balasubramanian, V., *Influence of Friction Stir Welding Process and Tool Parameters on Strength Properties of AA7075-T6 Aluminium Alloy Joints*, Mater. Des., **32**(2), pp. 535-549, Feb. 2011.

[31] Dehghani, K., Ghorbani, R. & Soltanipoor, A.R., *Microstructural Evolution and Mechanical Properties During The Friction Stir Welding of 7075-O Aluminum Alloy*, Int. J. Adv. Manuf. Technol., **77**(9-12), pp. 1671-1679, Apr. 2015.

[32] Maitra, S. & English, G.C., *Mechanism of Localized Corrosion of 7075 Alloy Plate*, Metall. Trans. A, **12**(3), pp. 535-541, Mar. 1981.

[33] Rao, T.S., Reddy, G.M. & Rao, S.R.K., *Microstructure and Mechanical Properties of Friction Stir Welded AA7075–T651 Aluminum Alloy Thick Plates*, Trans. Nonferrous Met. Soc. China, **25**(6), pp. 1770-1778, Jun. 2015.

[34] Mehri, A., Abdollah-zadeh, A., Habibi, N., Hajian, M. & Wang, J.T., *The Effects of Rotational Speed on Microstructure and Mechanical Properties of Friction Stir-Welded 7075-T6 Thin Sheet*, J. Mater. Eng. Perform., **29**(4), pp. 2316-2323, Apr. 2020.

[35] Tian, W., Li, S., Wang, B., Liu, J. & Yu, M., *Pitting Corrosion of Naturally Aged AA 7075 Aluminum Alloys with Bimodal Grain Size*, Corros. Sci., **113**, pp. 1-16, Dec. 2016.

[36] Heydarian, A. Dehghani, K. & Slamkish, T., *Optimizing Powder Distribution in Production of Surface Nano-Composite via Friction Stir Processing*, Metall. Mater. Trans. B, **45**(3), pp. 821-826, Jun. 2014.

[37] Tabasi, M., Farahani, M., Givi, M.K.B., Farzami, M. & Moharami, A., *Dissimilar Friction Stir Welding of 7075 Aluminum Alloy to AZ31 Magnesium Alloy Using Sic Nanoparticles*, Int. J. Adv. Manuf. Technol., **86**(1-4), pp. 705-715, Sep. 2016.